Control and Optimization of Grid-Tied Photovoltaic Storage Systems Using Model Predictive Control

Trudie Wang, Haresh Kamath, and Steve Willard

***Abstract*—In this paper, we develop optimization and control methods for a grid-tied photovoltaic (PV) storage system. The storage component consists of two separate units, a large slower moving unit for energy shifting and arbitrage and a small rapid charging unit for smoothing. We use a Model Predictive Control (MPC) framework to allow the units to automatically and dynamically adapt to changes in PV output while responding to external system operator requests or price signals. At each time step, the system is modeled using convex objectives and constraints and solved to obtain a control schedule for the storage units across the MPC horizon. For each subsequent time step, the first step of the schedule is executed before repeating the optimization process to account for changes in the operating environment and predictions due to availability of additional information. We present simulation results that demonstrate the ability of this optimization framework to respond dynamically in real time to external price signals and provide increased system benefits including smoother power output while respecting and maintaining the functional requirements of the storage units and power converters.**

***Index Terms*—Batteries, distributed power generation, distributed energy resources, dynamic pricing, energy management, energy storage, photovoltaic systems, power quality, power system control, smoothing, solar power generation.**

I. Introduction

ENVIRONMENTAL concerns and the need to find cleaner energy sources have resulted in the rapidly increasing penetration of Distributed Generation (DG) from renewable resources like solar. But as penetration of variable generation sources reaches and exceeds the 10–30% range, matching supply to load will begin to pose a significant challenge [1]–[4]. With such transformations looming in the near-future, energy storage will become crucial to creating a power system that can handle both the variability and unpredictability of renewable resources in an increasingly complex and diverse grid.

Photovoltaic systems directly coupled with battery energy storage (BES) are uniquely positioned to address these challenges. Such systems, when intelligently controlled, can integrate individual solar resources onto the grid while increasing system reliability and stability resources, thereby providing means for greater power system flexibility. For example, a grid tied PV storage system can be leveraged to address the supply-demand imbalance by using the BES for continuous bidirectional load balancing while also storing solar power for use when the sun is not shining. While the daily solar cycle and load follow the same general trend, the latter lags behind the former by a few hours and beyond 30% penetration, the greater impact of weather patterns on the current grid becomes a significant challenge for contingency power capacity and protection mechanisms to handle [5]. The excess output from local generation is absorbed by the storage system and is redelivered during shortfalls, making curtailment unnecessary and effectively firming up power from the PV array. By firming dispatch, reducing demand peaks and improving grid efficiency, BES displaces the amount of backup generation needed and offsets the need for fossil based spinning reserves and peaking resources in the dispatch stack. The dynamic response of BES located close to the solar resource can effectively act as a buffer to match the availability of generation to the draw from online loads, making solar a much more deployable resource. This is especially critical in low voltage networks with a high penetration of distributed renewables since the absence of buffering through either demand response (DR) or storage can result in large voltage variations, uncertainty of power flows, and possibly even reversed power flow to the transmission network which may impact local operation of the grid [4], [6]. PV storage systems can also exploit the rapid response of BES to handle the intermittency that results from cloud cover. When a cloud casts a shadow on the solar array, the storage unit automatically smoothes the output of the solar panels by instantaneously dispatching energy to fill in the drop created by the cloud. This increases the reliability of power from solar.

In this paper, we propose a dynamic and self-correcting framework that models the PNM Prosperity Energy Storage Project's on-premise BES and implements the intelligence and control logic to enable optimization and scheduling of the system. Located near Albuquerque, the PNM system provides 500 kW of power from solar panels directly coupled to 1 MWh rated battery capacity and is the first fully grid integrated solar storage facility in the US. With one of the largest combinations of PV and battery storage in the nation, the project aims to develop and demonstrate battery-storage technology that will create firm and dispatchable energy derived from a renewable energy source. The battery storage is separated into a high power 500 kW battery unit with added capacitors for rapid short term smoothing and a larger capacity 250 kW advanced lead acid battery unit to store and dispatch energy when needed. Currently, the system has demonstrated the ability to shift energy to peak periods and provide energy in rectangular blocks at predetermined demand schedules. It is simultaneously able to smooth PV output in reaction to recently experienced cloud cover.

Using Model Predictive Control (MPC), the optimization framework we propose can be used to model the PNM system and integrate various algorithms, objectives, constraints and forecast models into a policy that can be configured to the

Manuscript received February 13, 2013; revised September 20, 2013; accepted November 14, 2013. Date of current version February 14, 2014. This research was supported in part by the Electric Power Research Institute (EPRI) and by PNM Resources. Paper no. TSG-00112-2013.

T. Wang is with Stanford University, Stanford, CA 94305 USA (e-mail: trudie@stanford.edu).

H. Kamath is with the Electric Power Research Institute, Palo Alto, CA 94304 USA (e-mail: hkamath@epri.com).

S. Willard is with PNM Resources, Albuquerque, NM 87102 USA (e-mail: steve.willard@pnmresources.com).

Color versions of one or more of the figures in this paper are available online at http://ieeexplore.ieee.org.

Digital Object Identifier 10.1109/TSG.2013.2292525

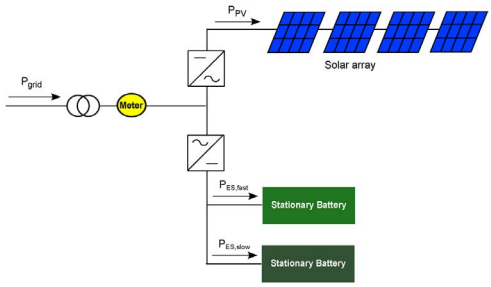

Fig. 1. Schematic representing grid tied PV storage system.

current operating environment. Because control is entirely local in MPC, there is no need for centralized grid management and the complexity of managing a decentralized, distributed network is made more tractable and reflective of local needs while leveraging local contribution of the distribution-level resources. To demonstrate the benefits of optimizing and dispatching the PNM PV-storage system using MPC, the model we develop will determine the ability of the BES to address intermittent local generation using ramping constraints while simultaneously shaping the power output profile of the system using price schedules. Showing this quantitatively will verify the system's ability to substitute for rapidly deployable backup generation as well as provide increased system flexibility and responsiveness to both local and system-wide intermittency and unpredictability. This will in turn show the potential of PV-storage to not only help in grid operating efficiency but also provides a significant amount of stability and resiliency to the power grid at times of sudden increase in demand or loss of generation and during times of fluctuating and intermittent solar power. The possibility for undesirable effects on the lifetime and functionality of the BES resulting from the optimized control policy will also be considered. This is examined by introducing an additional objective that penalizes excessive charging and discharging of the BES units. The aim is to see whether a mutually beneficial balance can be struck between the lifetime constraints of the BES and its contribution on the power grid. Finally, we compare these results to the prescient case to demonstrate MPC's ability to operate robustly and perform very near optimal. We show that a finite amount of information from the PNM system is sufficient to obtain a power profile that meets the required objectives while maintaining functionality and respecting system constraints.

The remainder of this paper is organized as follows. In Section II we provide the formal mathematical definition of the convex optimization problem used in our model, including the objectives and constraints of the storage units and the entire system. Section III describes the MPC method used to schedule and control the BES units in the grid tied PV storage system. Section IV then describes the method that is used to make PV output predictions at each time step within the MPC framework. In Section V we present the numerical details of our model and we follow this with a series of simulation results in Section VI using data taken from the PNM system to make MPC predictions. Finally, we conclude on our results in Section VII and discuss ideas about future work using the MPC framework.

II. Model

A. System Dynamics and Constraints

The PV storage system we model and simulate is shown schematically in Fig. 1. Within the system, the storage units and PV array each have an associated power schedule and negative power is always defined as power being generated and/or flowing out from the energy resource.

1) Photovoltaic (PV) Array: The PV array has a power schedule that is always negative since it only generates and does not consume power. Its output p_{PV} will fluctuate with changing climate and weather patterns and cannot be controlled. In our model, p_{PV} contributes to the system power balance and is predicted using historical profiles to enable scheduling of the storage units.

2) Battery Electric Storage (BES): Storage in our system is divided into two separate BES units, a large slower moving unit for energy shifting and arbitrage and a small rapid charging unit for smoothing. The larger BES unit holds the generated power from the PV array and uses it to hedge against high prices as well as act as a safeguard against unforeseen events on the power grid occur by dispatching energy when requested. The smaller BES unit acts more like a short-term buffer, rapidly shuttling energy in and out for short term smoothing. Since each unit can charge and discharge, their power schedules can be both positive and negative. The rates of charge and discharge are constrained by capacity limits. This is represented as $-D_{\mathrm{BES}}^{\max} \leq \hat{p}_{\mathrm{BES}} \leq C_{\mathrm{BES}}^{\max}$, where $D_{\mathrm{BES}}^{\max}$ and $C_{\mathrm{BES}}^{\max}$ are the discharging and charging rate limits and p_{BES} is the device power schedule.

The state of charge $q_{\mathrm{BES}}(t) \in \mathbf{R}^n$ of the n BES units is governed by the dynamics equation

$$q_{\mathrm{BES}}(t+1) = \eta_{BES}^{q} q_{\mathrm{BES}}(t) + \eta_{BES}^{p} p_{\mathrm{BES}}(t), \tag{1}$$

where $p_{\mathrm{BES}}(t) \in \mathbf{R}^n$ is the charging rate of the BES units at time t. $\eta_{\mathrm{BES}}^{q}, \eta_{\mathrm{BES}}^{p} \in \mathbf{R}^n$ lie in the interval [0,1] and are the storage and charging efficiencies. $qBES(t)$ must remain within the capacity limits of the battery, given as some fraction of the nominal capacity. We specify this as $Q_{\mathrm{BES}}^{\min} Q_{\mathrm{BES}}^{\mathrm{cap}} \leq q_{\mathrm{BES}}(t) \leq Q_{\mathrm{BES}}^{\max} Q_{\mathrm{BES}}^{\mathrm{cap}}$ where $Q_{\mathrm{BES}}^{\min}, Q_{\mathrm{BES}}^{\max} \in \mathbf{R}^n$ lies in the interval [0,1] and $Q_{\mathrm{BES}}^{\mathrm{cap}} \in \mathbf{R}^n$ contains the nominal ratings of the BES units.

3) Grid Connection: The PV storage system is tied to the grid at the point of common coupling (PCC) where power goes through a step up transformer before moving upstream to be converted from DC to AC. At this point, the power flow balance is modeled as

$$p_{\mathrm{grid}}(t) = p_{\mathrm{PV}}(t) + \mathbf{1}^T p_{\mathrm{BES}}(t), \tag{2}$$

where $p_{grid}(t)$ is the power schedule at the PCC at time t and can take on both positive and negative values. The term $\mathbf{1}^T \hat{p}_{\mathrm{BES}}(t)$ uses the vector of ones, $\mathbf{1}$, to sum the total flow from the BES units. A simple power limiter also caps the amount of power that can be transmitted over the line and we model this as $|p_{grid}(t)| \leq P_{\mathrm{PCC}}$ where P_{PCC} is the power limit at the PCC.

B. Objective

The system has two primary objectives, namely to provide energy arbitrage and to smooth intermittent output from the PV array. An additional secondary objective is also included to minimize excessive charge-discharge cycles of the BES units. The total cost incurred at each time step is denoted as $\ell(p_{\mathrm{grid}}(t), p_{\mathrm{BES}}(t))$, where $\ell : \mathbf{R}^{2n+1} \rightarrow \mathbf{R} \cup \{+\infty\}$ is a convex stage function. Because our objectives are distinct and separable, we can consider a stage cost function that is equal to the sum of the system objectives and the individual objectives,

$$\ell\left(\hat{p}_{\mathrm{grid}}(t), \hat{p}_{\mathrm{BES}}(t)\right) = \phi_{\mathrm{shift}}\left(\hat{p}_{\mathrm{grid}}(t)\right) + \phi_{\mathrm{smooth}}\left(\hat{p}_{\mathrm{grid}}(t)\right) + \phi_{\mathrm{cyc}}\left(\hat{p}_{\mathrm{BES}}(t)\right), \tag{3}$$

where the $\hat{}$ operator is used to denote an estimated state or quantity at times when the value is unknown. The first term,

$\phi_{\text{shift}}(\hat{p}_{\text{grid}}(t))$, represents shifting energy for arbitrage. Because the system we model is a net generator of power, this term is a negative cost i.e. a profit. While there are many methods to achieve shifting, the most practical and effective technique is to simply use real-time wholesale pricing since this allows both consumers and providers to participate and benefit from power transactions as the power grid develops into a more dynamic and responsive system [10]–[13]. Although such real time price schedules are not currently deployed at all levels of the grid, many utilities are moving towards prices that reflect the actual cost of power especially as the technologies for communicating these prices becomes more common and widespread. We thus represent the shifting term as $\phi_{\text{shift}}(\hat{p}_{\text{grid}}(t)) = c(t)\hat{p}_{\text{grid}}(t)$, where $c(t)$ is the energy price at time t. The second term, $\phi_{\text{smooth}}(\hat{p}_{\text{grid}}(t))$, is the cost associated with the smoothness of the grid output. For this term, we consider a weighted sum of three different measures of smoothness to account for the maximum range, slope and curvature of the power output. This minimizes the variation in magnitude and rate of change of the output to produce a more consistent and smoother power profile.

We represent this term as

$$\begin{aligned}\phi_{\text{smooth}}(\hat{p}_{\text{grid}}(t)) = {} & \alpha_{\text{range}}(\max \hat{p}_{\text{grid}} - \min \hat{p}_{\text{grid}}) \\ & + \alpha_{\text{diff}} \left|\hat{p}_{\text{grid}}(t) - \hat{p}_{\text{grid}}(t-1)\right| \\ & + \alpha_{\text{curv}} \left(\hat{p}_{\text{grid}}(t-1) - 2\hat{p}_{\text{grid}}(t) \right. \\ & \left. + \hat{p}_{\text{grid}}(t+1)\right)^2,\end{aligned}$$

where $\alpha_{\text{range}}, \alpha_{\text{diff}}$ and α_{curv} are the penalty parameters for tuning the range, slope and curvature terms respectively.

The final term, $\phi_{\text{cyc}}(\hat{p}_{\text{BES}}(t))$, adds a penalty for excessive charging and discharging. We represent this term as $\phi_{\text{cyc}}(\hat{p}_{\text{BES}}(t)) = \alpha_{\text{BES,cyc}}|\hat{p}_{\text{BES}}(t) - \hat{p}_{\text{BES}}(t-1)|$, where $\alpha_{\text{BES,cyc}}$ is the cycling penalty parameter. This non-negative cycling cost is similar to the slope term used for the smoothing objective and ensures that system operation costs are balanced against the functionality and lifetime costs of the BES units. Note that $\phi_{\text{cyc}}(\hat{p}_{\text{BES}}(t))$ is shown to depend on all batteries. This is because we give both BES units the freedom to charge and discharge for any objective. Differentiating the BES units for specific objectives is unnecessary since the optimization process chooses the most suited unit to either smooth or shift power [14].

An important point to emphasize is that the stage cost ℓ is not assumed to be known in advance. Uncertainties in exogenous input and unknown intrinsic system variables are incorporated into ℓ through predictions and forecasts. The overall objective of the system is the average stage cost across all time,

$$J = \lim_{T\to\infty} \frac{1}{T} \sum_{t=0}^{T-1} \ell\left(\hat{p}_{\text{grid}}(t), \hat{p}_{\text{BES}}(t)\right). \tag{4}$$

C. Control Policy

The control policy in our PV storage system selects the control variables based on information available at the current time t. Known information includes system device parameters and grid line limits as well as measured quantities. This information along with external wholesale prices and estimates of unknown quantities are then used to calculate the future stage costs and minimize the total cost. Through this optimization process, the policy to determine the power schedules of each BES unit.

III. Method

Model predictive control (MPC) is a control policy that allows us to set up a framework that we use to dynamically and robustly control and schedule the PV storage system. Within the MPC framework, the model of our system from Section II is solved as an optimization problem in real time at each time step to determine an action policy and enable scheduling of each BES unit over the finite MPC time horizon. The controller uses predictions based on historical data to help determine the local control actions of each device. Although a formal statistical or stochastic model can be used to represent uncertainty when making predictions, it is not needed for the policy to work and the controller can often perform very robustly even when predictions are poor [15].

The first step in MPC is to solve the optimization problem at the current time step τ and determine conditional power schedules for each BES unit over a fixed time horizon extending T steps into the future. The solver uses the information available to it locally along with predictions of unknown quantities to minimize the MPC objective function subject to the constraints of the BES units and power converters as well as the constraints at the PCC. The optimization problem we solve is similar to the one specified in Section II but over a finite time horizon,

$$\begin{aligned}\underset{\hat{p}_{\text{grid}}(\tau),\hat{p}_{\text{BES}}(\tau)}{\text{minimize}} \quad & \frac{1}{T}\sum_{\tau=t}^{t+T-1} \hat{\ell}\left(\hat{p}_{\text{grid}}(\tau), \hat{p}_{\text{BES}}(\tau)\right) \\ \text{subject to} \quad & \hat{p}_{\text{grid}}(\tau) + \hat{p}_{\text{PV}}(\tau) + \mathbf{1}^T\hat{p}_{\text{BES}}(\tau) = 0 \\ & \left|p_{grid}(\tau)\right| \le P_{\text{PCC}} \\ & \hat{q}_{\text{BES}}(\tau+1) = \eta^q_{BES}\hat{q}_{\text{BES}}(\tau) \\ & + \eta^c_{BES}\left(\hat{p}_{\text{BES}}(\tau)\right)_+ + \left(\frac{1}{\eta^d_{BES}}\right)\left(\hat{p}_{\text{BES}}(\tau)\right)_- \\ & Q^{\min}_{\text{BES}}Q^{\text{cap}}_{\text{BES}} \le \hat{q}_{\text{BES}}(\tau) \le Q^{\max}_{\text{BES}}Q^{\text{cap}}_{\text{BES}} \\ & -D^{\max}_{\text{BES}} \le \hat{p}_{\text{BES}}(\tau) \le C^{\max}_{\text{BES}} \\ & \hat{q}(\tau) = q(\tau), \quad \hat{q}(\tau+T) = q_{\text{final}} \\ & \tau = t, \ldots, t+T-1,\end{aligned} \tag{5}$$

where $(z)_+ = \max(0, z)$ and $(z)_- = \min(0, z)$. The $\hat{}$ operator indicates an estimated state or quantity at time step τ with $\tau|t$ denoting an estimate of a quantity at time τ based on information available at current time t. T is the MPC time horizon over which we schedule the storage units. A terminal constraint has additionally been added to the BES units to ensure that the storage system is not depleted at the end of the time horizon, with a common choice of q_{final} being $0.5Q_{cap}$ or the initial charge state of the battery.

In order to avoid oscillations between MPC iterations, we have also added a regularization term to our objective function which we specify as $\phi_{prev} = \gamma_{\text{prev}}\|\hat{p}_{\text{grid}} - \hat{p}^{\text{prev}}_{\text{grid}}\|^2_2$, where $\hat{p}^{\text{prev}}_{\text{grid}}$ is the solution for the previous iteration and γ_{prev} is the damping weight for oscillations between iterations. This prevents the solution at the current time step from diverging too far from the previous time step and ensures that smoothness across the MPC prediction horizon does not come at a cost to smoothness between the current time step and the previous time steps.

At time t, the optimization problem subject to all constraints is solved with the predicted values and $\hat{p}(t)^\star, \ldots, \hat{p}(t+T)^\star$ forms the optimal solution to the MPC problem over the time horizon T. The first step of the determined power schedules are then executed before the solution at the next time step updates the control policy using $p(t) = \hat{p}(t)^\star$ along with any new information and forecasts. Each storage unit then executes the first step of its schedule and repeats the optimization process, incorporating changes in operating environment, as well as new measurements and external information that may have subsequently become available [9], [16]. The process of acquiring new information, making predictions and optimizing is repeated at every time step

thereafter to ensure that the solution is robust to measurement errors, missing information and inaccurate forecasts. This iterative process allows the storage units to adjust their schedules in response to external disturbances that were unknown at the time the schedules were computed and ensures that the control policy dynamically adapts as new information arrives and changes in the operating environment occur [9], [16], [17].

While the dynamics of the storage units can be represented using a more complex system of equations and these can be readily integrated into the MPC framework, in this paper we use a simple dynamics model to demonstrate that MPC performs well in real-time even with limited computational resources and measurements. Since MPC is self-correcting and forecasting is carried out at every time step with refitted parameters using updated information, a model that generally represents the dynamics of the devices is adequate. MPC also directly handles objectives and constraints without having to learn and adjust controller parameters via a trial and error process, and this makes it particularly well suited for rapid real-time optimization of a locally controlled system which is dependent on the operating environment. The fact that both our objective and constraints are convex means the problem can be solved very efficiently and while MPC is a heuristic policy that is generally not optimal, it often performs far superior to traditional control methods ([18]–[20]). Recent advances in convex optimization give embedded processors in power conversion devices the potential to perform calculations efficiently in the millisecond and microsecond time scales [8], [17], [21]. The combination of a rapid open source convex solver that handles objectives and constraints directly [21], [22] and increasing CPU capabilities enables power schedules to be dynamically computed. Additionally, offline simulations using different control policies can be benchmarked on similar time scales prior to online implementation. In cases where the objectives and constraints are nonconvex, good local solutions can also be obtained using various techniques such as sequential convex programming ([23]–[25], [37]).

Another important characteristic of the MPC framework is that it only requires *local* predictions to determine control actions for the storage units and does not use estimates from any other part of the power network other than what can be measured at the PCC. Optimization is independent of the rest of the grid and this allows for autonomous operation with minimal coordination with other agents. Independent, bottom-up control not only reduces the communication requirements but also makes it feasible to connect large numbers of these distributed systems to the grid without requiring the implementation of complex top-down control systems. This paradigm shift suggests a new way to think of operating the grid. In such a multi-agent coordination system, each system can optimize local control while still using external price signals as an input to help the power grid achieve system-wide objectives. The incorporation of external signals essentially allows each system to align locally optimized operating policies with the needs of the entire system. Distributing the optimization among the agents allows the complexity of an individual system's control effort to remain low while the coordinated effort allows for an emergent intelligence. The computational requirements are significantly reduced by leveraging local control efforts.

IV. Predictions

Estimates of unknown input variables are required at each time step in MPC in order to solve the optimization problem and determine a control policy over the finite time horizon. These estimates can be based on historical data, stochastic models, load and weather forecasts, and pricing information. While many methods have been used to predict energy profiles on the power grid, ranging from multiple regression to expert systems [26]–[28] and total load over a large region can be predicted up to 1% accuracy, predicting generation locally from intermittent renewable resources poses a greater challenge due to nuances that require detailed knowledge of the system environment and geographic diversification cannot smooth out. The versatility of MPC means that it is not tied to any specific forecasting method and can incorporate a range of techniques depending on what information can be accessed. Because the method recalculates its schedule at each time step after executing the first step of the schedule, it dynamically adjusts itself and is self-correcting. This means that perfect predictions are not required for the method to perform robustly and predictions that capture general future trends are sufficient ([15]).

For our grid tied PV storage system, we incorporate predictions into the stage cost ℓ for the output of the PV array. To predict PV output, we require only local measurements of historical output since the system just needs to forecast its own future generation profile in each MPC time period. We denote the historical PV output data as $p_{\mathrm{PV}}^{\mathrm{hist}} \in \mathbf{R}_{\mathrm{hist}}^{T}$ where T_{hist} is the historical time horizon and assume that the data has general periodicity over a 24 hour period. This is a good assumption over a period of a few days where the seasonal variation is insignificant since the solar insolation at any geographical location and given time is well determined. Deviations from the expected PV array output are due to weather conditions like cloud cover that result mostly in drops in output with occasional over-irradiance due to cloud enhancement effects. This leads us to propose an asymmetric least squares fit of the available historical PV output data to provide a periodic baseline that is weighted towards the outer envelope of the observed data. To generate the PV output prediction, we first determine the historical baseline $\hat{p}_{\mathrm{PV}}^{\mathrm{hist}}$ by solving an approximation problem with a smoothing regularization term and a periodicity constraint,

$$\begin{aligned}
\underset{\hat{p}_{\mathrm{PV}}^{\mathrm{hist}}}{\text{minimize}} \quad & \frac{1}{T}\sum_{\tau=t-T_{\mathrm{hist}}+1}^{t-1}\Bigg(\left(\hat{p}_{\mathrm{PV}}^{\mathrm{hist}}(\tau)-p_{\mathrm{PV}}^{\mathrm{hist}}(\tau)\right)_{+}^{2} \\
& \qquad +\gamma_{\mathrm{asym}}\left(\hat{p}_{\mathrm{PV}}^{\mathrm{hist}}(\tau)-p_{\mathrm{PV}}^{\mathrm{hist}}(\tau)\right)_{-}^{2} \\
& \qquad +\gamma_{\mathrm{curv}}\Big(\hat{p}_{\mathrm{PV}}^{\mathrm{hist}}(\tau-1)-2\hat{p}_{\mathrm{PV}}^{\mathrm{hist}}(\tau) \\
& \qquad\qquad +\hat{p}_{\mathrm{PV}}^{\mathrm{hist}}(\tau+1)\Big)^{2}\Bigg) \\
\text{subject to} \quad & \hat{p}_{\mathrm{PV}}^{\mathrm{hist}}(\tau)=\hat{p}_{\mathrm{PV}}^{\mathrm{hist}}(\tau+T_{\mathrm{period}}) \\
& \tau=t-T_{\mathrm{hist}}+1,\ldots,t-1, \qquad (6)
\end{aligned}$$

where γ_{asym} and γ_{curv} represent the weights for the asymmetric and curvature terms respectively. The first and second term of the objective function represent the positive and negative deviation of the predicted curve from the actual data and the third term smooths the curvature in the predicted curve. The first term is weighted more heavily to push the predicted curve towards the outer envelope of the fluctuating data. The constraint ensures periodicity across $T_{\mathrm{period}} = 24$ hrs. Solving this problem de-noises the data to reconstruct a smooth baseline profile [19]. The objective function is a weighted sum of squared convex terms and forms a regularized convex problem which trades off an asymmetric least-squares fit against the mean-square curvature of the data. The baseline prediction for the MPC horizon is then defined as $\hat{p}_{\mathrm{PV}} = \hat{p}_{\mathrm{PV}}^{\mathrm{hist}}(t-T_{\mathrm{period}},\ldots,t+T-T_{\mathrm{period}})$.

Once we determine this baseline prediction, we correct for transient weather phenomena by adjusting the baseline using an error fit with a linear model applied to the residual $r = \hat{p}_{\mathrm{PV}}^{\mathrm{hist}} - p_{\mathrm{PV}}^{\mathrm{hist}}$. The correction is calculated by writing the predicted residual at the time step τ as a weighted sum of the previous residuals, $\hat{r}(\tau) = a_1 r_{\tau-1} + a_2 r_{\tau-2} + \cdots + a_n r_{\tau-n}$ where a is an n-element vector determining what weights to give the n previous residuals. The associated residual prediction error is defined as $e(\tau) = \hat{r}(\tau) - r(\tau)$. To determine a, we minimize the sum of the squared l_2 norms of the prediction error over the entire historical data time horizon $\tau = t - T_{\mathrm{hist}} + 1, \ldots, t-1$. We can rewrite this concisely in matrix form,

$$\|e\|_2^2 = \|Ma - b\|_2^2 \tag{7}$$

where $b = \begin{bmatrix} r(n+1) \\ r(n+2) \\ \vdots \\ r(T_{\mathrm{hist}}) \end{bmatrix}$,

$$M = \begin{bmatrix} r(n) & r(n-1) & \vdots & r(1) \\ r(n+1) & r(n) & \vdots & r(2) \\ \vdots & \vdots & \vdots & \vdots \\ r(T_{\mathrm{hist}}-1) & r(T_{\mathrm{hist}}-2) & \vdots & r(T_{\mathrm{hist}}-n) \end{bmatrix}$$

This is a least squares problem and has the analytical solution $a = M^{\dagger} b$ where the † symbol denotes the Moore-Penrose pseudoinverse. We assume M is full rank since the residuals are due to random weather patterns and can effectively be treated as independent and identically distributed. The predicted residual corrections across the MPC horizon are then decreased by a factor λ at each future time step, where $0 < \lambda < 1$. This reduces the magnitude of the correction over the MPC horizon moving forward in time so that the prediction reverts back to the baseline. The procedure used to make predictions at each MPC time step is summarized in Algorithm 1.

Algorithm 1 Computing PV predictions from historical data.

1: Compute baseline profile $\hat{p}_{\mathrm{PV}}^{\mathrm{hist}}$ over MPC horizon using $p_{\mathrm{PV}}^{\mathrm{hist}}$ to solve (6).
2: Compute residual $r = \hat{p}_{\mathrm{PV}}^{\mathrm{hist}} - p_{\mathrm{PV}}^{\mathrm{hist}}$.
3: Determine the residual weights a by (7).
4: Compute predicted residuals over MPC horizon as $\hat{r}(\tau) = \lambda^{\tau-t} a^T [r(\tau-1) \cdots r(\tau-n)]$ for $\tau = t, \ldots, t+T$.
5: Compute prediction as $\hat{p}_{\mathrm{PV}} + \hat{r}$.

The adaptability of MPC means that the adjusted least squares fit of the PV output data is able to handle uncertainties and provide sufficiently accurate forecasts to enable dynamic power scheduling. This prediction method is simple to implement using available historical data and requires very little computational effort during real time implementation. While we can use a similar method with comparable accuracy for predicting real-time prices using historical wholesale price data available to market participants, we use the exact price in our simulations since currently available wholesale prices on the power grid are determined and provided in hourly time steps 24 hrs in advance.

V. Numerical Example

We demonstrate the dynamic and adaptive capabilities of the MPC algorithm on a grid tied PV storage system using data and specifications taken from the PNM Prosperity Energy Storage Project in New Mexico [29]. The PNM system is one of the largest grid tied PV storage systems in the US, providing 500 kW of power from solar panels which are directly coupled to battery storage capable of providing up to 750 kW. The battery storage is separated into a rapid 500 kW Ultra battery unit for rapid short term smoothing and a 1000 kWh, 250 kW advanced lead acid battery unit to store and dispatch energy when needed.

TABLE I
PNM Parameters

Parameter	Description	Value
$P_{\mathrm{PCC}}^{\max}$	Maximum power output of PNM system	1250kW
$P_{\mathrm{PV}}^{\max}$	Maximum power output of PV array	500kW
$C_{\mathrm{BES},1}^{\max} = D_{\mathrm{BES},1}^{\max}$	Maximum charge and discharge rate of large BES unit	250kW
$C_{\mathrm{BES},2}^{\max} = D_{\mathrm{BES},2}^{\max}$	Maximum charge and discharge rate of small BES unit	500kW
$Q_{\mathrm{BES},1}^{\mathrm{cap}}$	Nominal storage capacity of large BES unit	1000kWh
$Q_{\mathrm{BES},2}^{\mathrm{cap}}$	Nominal storage capacity of small BES unit	180kWh
$\eta_{BES,1}^{p}$	Charge efficiency of large BES unit	0.70
$\eta_{BES,2}^{p}$	Charge efficiency of small BES unit	0.95
$\eta_{BES,1}^{q}$	Leakage efficiency of large BES unit	1.00
$\eta_{BES,2}^{q}$	Leakage efficiency of small BES unit	1.00

The PNM system is connected to the grid at the PCC through a power converter with a bidirectional meter and control system which has access to real-time prices. The connection also has a physical power transfer limit $P_{\mathrm{grid}}^{\max} = 1250$ kW. The system takes measurements and data at 1 second intervals at all points of the system, including the power output of the PV array and the output at the PCC. We incorporate this into the model described in Section II as historical data and use MPC to enable optimization and scheduling of the BES units. Since the maximum output of the PV array is 500 kW, any excess solar insolation falling on the array must be dumped. For this reason, we use the power output measurements for predictions of future PV output instead of insolation and temperature measurements since they more accurately represent the output to the system.

The 500 kW and 250 kW BES units have 180 kWh and 1000 kWh storage capacity respectively. The charging rate $C_{\mathrm{BES}}^{\max}$ and discharging rate $D_{\mathrm{BES}}^{\max}$ are assumed to be equivalent. The efficiencies are based on information provided to us from the battery manufacturers of the system batteries. The large difference in the charge efficiency values is due to the fact that the smaller battery uses a different technology which makes it more efficient for high capacity power transfers but also makes it much more costly per unit of capacity. Since the leakage efficiencies are near unity, we use 1 for both units. We choose the initial state of each BES unit to be 50% of the nominal capacity. The parameters of each unit along with the system specifications and parameters are summarized in Table I below.

The simulations are run using data taken from the time period July 17–24, 2012. These days were selected to ensure the climate was warm enough to warrant demand shifting and increased prices at peak hours while also incorporating a period of cloud cover where intermittency would provide a need for smoothing PV output. For the simulation period, we use day-ahead hourly wholesale price data published by the CAISO [30]. We chose to use the CAISO data since PNM currently does not publish dynamic electricity rates and the climate and load shapes in New Mexico are reasonably close to those found in southern California to warrant similar price schedules. Also, while wholesale price schedules are not currently used by all systems at the distribution level, we elected to use wholesale prices since they are best positioned to allow consumers and generators to participate and benefit from power transactions as the power grid develops into a more dynamic and responsive system [10]–[13].

For each scenario we simulate, we use an MPC time horizon of $T = 180$. This corresponds to 4 minute intervals over a 12 hour

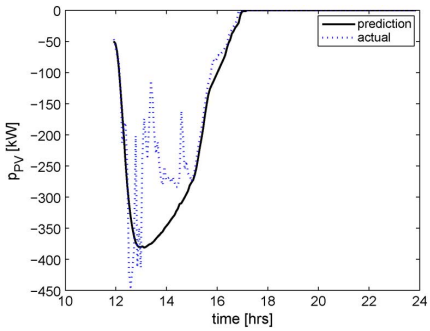

Fig. 2. Predicted PV output over a 12 hour period at 12 PM on July 17, 2012.

period and is a typical time step and horizon for price signals and DR. The time step $t = 1$ corresponds to midnight.

VI. Results

To demonstrate how the PV storage system can dynamically and automatically respond to various objectives including smoothing system output and using real-time prices for shifting, we present simulation results for a range of scenarios. Each scenario is evaluated with metrics for cost of shifting, smoothing and lifetime of the BES units. The cost of shifting is simply the area under the $c(t)p_{\text{grid}}(t)$ curve and we use a straightforward trapezoidal approximation to determine the cost,

$$\Phi_{\text{shift}} = \sum_{t=1}^{T_{\text{f}}-1} \frac{1}{2}\left(c(t)p_{\text{grid}}(t) + c(t+1)p_{\text{grid}}(t+1)\right) dt,$$

where $T_{\text{f}} = 1800$ is the simulation end time and $dt = 4$ minutes. For the smoothing cost, there is as of yet no consensus on how to measure and price intermittency. Since system operators are mainly concerned with rates of change of power, we use a metric that represents the cumulative sum of the absolute values of the curve slope. This is a normalized version of the slope term in our smoothing objective and is similar to what was used in the PNM interim report [31],

$$\Phi_{\text{smooth}} = \frac{\sum_{t=1}^{T_{\text{f}}-1} \left|p_{\text{grid}}(t+1) - p_{\text{grid}}(t)\right|}{\sum_{t=1}^{T_{\text{f}}-1} \left|p_{\text{PV}}(t+1) - p_{\text{PV}}(t)\right|}.$$

There is also lack of consensus on how to measure the lifetime impact on the BES units, since it is difficult to determine the different effects of deep and shallow cycling. There is general agreement, however, that lifetime degradation is strongly correlated to the amount of energy that has been moved in and out of the battery terminals. This is equivalent to the area under the $|p_{\text{BES}}|$ curve and again we use the trapezoidal approximation to determine the cost,

$$\Phi_{\text{cyc}} = \sum_{t=1}^{T_{\text{f}}-1} \frac{1}{2}\left|p_{\text{BES}}(t) + p_{\text{BES}}(t+1)\right| dt.$$

The wholesale price and PV output during the simulation time period are added onto the historical data incrementally at each time step and used to update the MPC predictions. The predictions are made using 5 days of historical data to predict the next 12 hours of generation. An example of a prediction during an intermittent period between 12 PM to 12 AM is shown in Fig. 2. As can be observed, the error correction pulls the baseline towards the actual output. This ensures that the shape of the prediction closely matches the PV output at each time step.

The α weights on the individual objectives are determined by varying each one across an extensive range of values and finding the combination that minimizes the total system cost.

TABLE II
Cost Metrics for Simulated Scenarios

Scenario	Φ_{shift}[\$/kWh]	Φ_{smooth}	Φ_{cyc}[kWh]
base case (PV output)	−4892	1.000	–
smoothing	−4917	0.3920	3044
shifting	−5053	1.740	3971
smoothing and shifting	−5017	0.6674	3635
smoothing and shifting (prescient)	−5031	0.3052	3678
smoothing, shifting and BES cycling	−5040	0.9141	2710

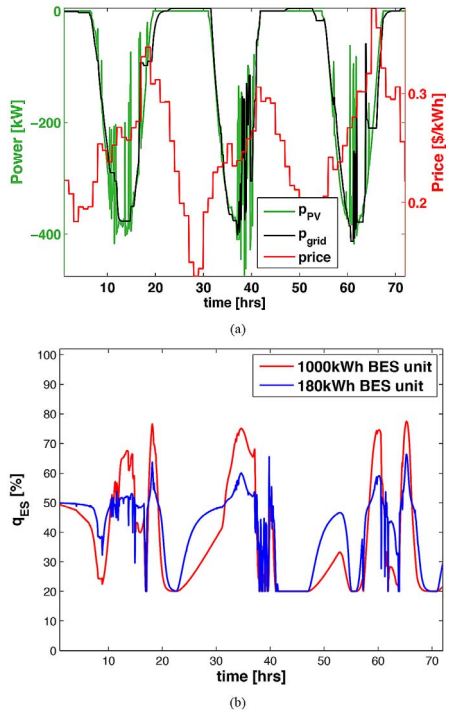

Fig. 3. Grid output (*top*) and BES units SOC (*bottom*) plotted over the simulation time horizon for the smoothing objective.

For each scenario simulated, we provide the cost metrics in Table II. The *base case* refers to the scenario where the grid output profile is not modified, i.e. is equal to the PV output. We also provide the simulated output and power schedules of the system and BES units for the first 3 days of some of the scenarios. We present a selection of our resuls in Figs. 3 and 4, with the first plot in each figure representing the PV and grid output with a green solid line and black dotted line respectively. In the second plot, the large and small battery SOCs are represented by the red solid line and blue dotted line.

We begin by examining the effect of each system objective independently. The smoothing objective results in p_{grid} being notably smoother and steadier than p_{PV}. This is clearly seen in Fig. 3. Contrasting this *smoothing only* scenario with the base case, Φ_{smooth} is reduced by 60.8%. Not surprisingly, most of the high frequency smoothing is allocated to the small BES unit since it is able to respond more rapidly. The larger BES unit primarily handles the lower frequency diurnal swings of the solar resource, using its greater capacity to store the energy and provide it when necessary to help with smoothing the grid output.

Since the main price peak occurs at around 6 PM each day and is preceded several hours by the solar peak at around 12 PM, the BES units in the *shifting only* scenario are used for arbitrage and shift the PV output towards the peak price times. System output increases rapidly right before each peak price occurs as the storage system discharges to take advantage of the day ahead price schedule. Similarly, low prices result in the BES units quickly charging using power from the PV array and this

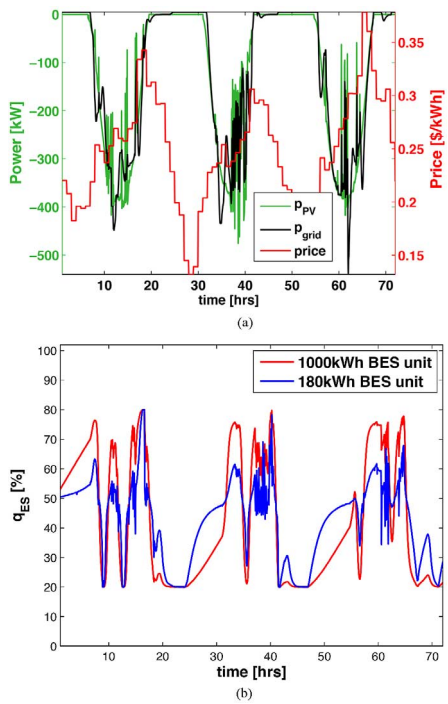

Fig. 4. Grid output (*top*) and BES units SOC (*bottom*) plotted over the simulation time horizon for simultaneous smoothing and shifting.

results in rapid drops in total system output. The price is effectively shifting the output of the system through economic incentive. In this scenario the batteries have only the price objective to work towards and so as expected both units act similarly in their charging and discharging behavior in order to maximize profit for the system. The slight variations in charging and discharging are due to the differences in efficiency as well as the maximum charging and discharging capacities of the units. Again comparing to the base case, Φ_{shift} in this *shifting only* scenario drops (profit increases) by 3.29%.

We next simulate the *smoothing and shifting* scenario in which the PV storage system simultaneously provides both smoothing and shifting. The α weights on the objectives are adjusted to provide and demonstrate an appropriate trade off between the two objectives. When responding only to price, the BES units tend to discharge and charge rapidly in a knee-jerk fashion in order to maximize profit. We dampen the power swings by increasing the relative weights on the smoothing objectives. The grid output shown in Fig. 4 demonstrates this scenario in which the BES units are simultaneously able to shift output to peak price times while smoothing PV output in anticipation of forecasted cloud cover. Comparing the metrics, the decrease in Φ_{smooth} drops by 45.3% relative to the *smoothing only* scenario and the decrease in Φ_{shift} drops by 22.4% when compared to the *shifting only* scenario. But both Φ_{smooth} and Φ_{shift} are still significant improvements from the base case and are able to garner a 33.3% and 2.56% improvement respectively. Note that when the objective is both smoothing and shifting, the optimization algorithm at each MPC time step automatically assigns the small BES unit with a more rapid response to handle most of the smoothing while using the slower larger BES unit to shift PV output.

We also compare this scenario to the prescient case where instead of using predictions, we assume prescient knowledge of PV output over the MPC horizon. While MPC is only a heuristic policy and hence does not guarantee optimality, it generally demonstrates results that are close to optimal and comparing MPC to the prescient case helps illustrate this. Even with our simple forecasting methods, Φ_{shift} only increases by 11.2% relative to the gain from the prescient case. This performance is not echoed in Φ_{smooth} however. The decrease in this metric approximately doubles the gain of the prescient case. The reason for this discrepancy in performance lies in how the PV predictions are made. Since we rely only on historical power profiles, our predictions are able to capture periodic trends and peaks very accurately. But without external forecast data, it is not possible to adequately capture transient weather phenomena like cloud cover since historical data does not inherently represent such random chaotic events. Φ_{shift} is able to come much closer to the prescient value than Φ_{smooth} because profits from shifting depend primarily on general periodic trends while the ability to smooth output relies on knowledge of transient weather phenomena to offset rapid unpredictable changes. There is still a significant improvement in Φ_{smooth} from the base case but the results suggest that smoothing has much more to gain from supplementing historical data with external weather forecasts to make PV output predictions. While we included an ARMA correction to account for sudden changes in PV output and ensure immediate response to sudden changes in weather patterns, performance could be greatly improved if some form of weather prediction was included in the data used to forecast the PV profile. PNM is still actively working on acquiring this data but because of the flexibility of our prediction method, it is trivial to incorporate such data by including an additional weighted term to the asymmetric least squares objective once it becomes available and this should greatly improve the smoothing capabilities of the MPC algorithm.

When a BES cycling cost is added to the system objective functions, we see an increase in Φ_{smooth} by about 37.0%. This is in exchange for a reduction in Φ_{cyc} by about 25.4%. A particularly interesting result of introducing the battery cycling cost is that it not only causes Φ_{smooth} to increase in order to decrease Φ_{cyc}, but it also incidentally causes Φ_{shift} to decrease slightly by about 0.46%. This demonstrates how MPC can balance the independent objectives to enable acceptable trade offs to be determined and implemented within a PV storage system when issues like battery lifetime are important and the impact of cycling can be quantified.

A. Computation Times

The simulation is carried out using CVX [20] to solve the optimization at each time step. CVX is a modeling system that solves convex optimization problems by converting them into semidefinite programs (SDPs). Using open-source solvers, it runs in a Matlab environment and is hence ideal for rapid code development and deployment. Since MPC uses the first step of the previous solution to provide a warm start for the next iteration, the optimization problem at each MPC iteration can be solved on an Intel Xeon 3.0 GHz dual core processor in approximately 4 seconds. The predictions at each time step are similarly solved using CVX and require an additional 7 seconds. This means that the amount of time required at each MPC step will be significantly less than the amount of time lapsed between MPC time steps, making real time dynamic solutions entirely feasible. While this demonstrates that our methods are suitable for real-time implementation, we were carrying out simulations using a scripted language as a proof of concept before actual implementation using embedded code. Hence the times reported are conservative approximations only and significantly better performance times can be attained using CVXGEN [21] or similar

tools to generate custom embedded solvers for deployment on embedded processors.

VII. Conclusion

In this paper, we have tackled the challenge of controlling and coordinating BES units in a PV storage system for smoothing the intermittency of the solar resource and shifting output to more closely match the load profile. The PV storage system is modeled as a convex optimization problem and an MPC framework solves the optimization problem using external price signals and predictions of PV output at each time step. Our prediction consists of an asymmetric least squares fit of the PV output data with a linear error correction to handle uncertainties and provide forecasts to enable dynamic power scheduling. This method is sufficiently accurate given the adaptability and self-correcting nature of the MPC algorithm. To demonstrate the performance of the MPC method and its ability to schedule the BES units, we have simulated and compared a number of scenarios using real-time data taken from the PNM Prosperity Energy Storage Project. We show that using only locally available information, MPC can schedule the BES units to accommodate various objectives and help to balance trade-offs between smoothing intermittent local generation, shifting output in response to price signals and maintaining the functional requirements of the BES units and power converters. Extensive cost savings are attainable with all cost metrics and the performance is shown to come very close to the prescient scenario. The MPC framework we have developed will be extended to explore interactions between BES units in scenarios where grid constraints and different shifting and smoothing requirements create additional demands on the system, as well as explore how various forecasting and scheduling algorithms can be used to meet these demands while still minimizing cost to the system.

Acknowledgment

The authors thank Eric Chu, Matt Kraning and Dan O'Neill for extensive discussions on the problem formulation and prediction methods and Stephen Boyd for his advising and guidance on the problem formulation and prediction methods.

References

[1] J. Barton and D. Infield, "Energy storage and its use with intermittent renewable energy," *IEEE Trans. Energy Convers.*, vol. 19, pp. 441–448, Jun. 2004.

[2] D. T. Ton, C. J. Hanley, G. H. Peek, and J. D. Boyes, "Solar energy grid integration systems—Energy storage (SEGIS-ES)," Sandia National Laboratories, Jul. 2008.

[3] P. Denholm, E. Ela, B. Kirby, and M. Milligan, "The role of energy storage with renewable electricity generation," National Renewable Energy Laboratory, Rep. TP-6A2-47187, 2010.

[4] C. Whitaker, J. Newmiller, M. Ropp, and B. Norris, "Distributed photovoltaic systems design and technology requirements," Sandia National Laboratories, 2008.

[5] M. P. Richard Perez and T. E. Hoff, "Quantifying the cost of high photovoltaic penetration," in *Proc. SOLAR 2010 Conf. Amer. Solar Energy Soc.*.

[6] E. Liu and J. Bebic, "Distribution system voltage performance analysis for high-penetration photovoltaics," National Renewable Energy Laboratory, 2008.

[7] Y. Wang and S. Boyd, "Fast model predictive control using online optimization," in *Proc. IFAC World Congr.*, Jul. 2008, pp. 6974–6997.

[8] J. Mattingley, Y. Wang, and S. Boyd, "Code generation for receding horizon control," in *Proc. IEEE Multi-Conf. Syst. Control*, Sep. 2010, pp. 985–992.

[9] A. Bemporad, "Model predictive control design: New trends and tools," in *Proc. 45th IEEE Conf. Decision Control*, 2006, pp. 6678–6683.

[10] A. Faruqui and S. Sergici, "Household response to dynamic pricing of electricity: A survey of the experimental evidence," Brattle Group, 2009.

[11] C. Goldman, N. Hopper, O. Sezgen, M. Moezzi, and R. Bharvirkar, "Customer response to day-ahead wholesale market electricity prices," Lawrence Berkeley National Laboratory, 2004.

[12] N. Hopper, C. Goldman, and B. Neenan, "Demand response from day-ahead hourly pricing for large customers," 2006.

[13] S. Borenstein, M. Jaske, and A. Rosenfeld, "Dynamic pricing, advanced metering, and demand response in electricity markets," 2002.

[14] M. Kraning, Y. Wang, E. Akuiyibo, and S. Boyd, "Operation and configuration of a storage portfolio via convex optimization," 2011.

[15] Y. Wang and S. Boyd, "Performance bounds for linear stochastic control," *Syst. Control Lett.*, vol. 53, pp. 178–182, Mar. 2009.

[16] J. Maciejowski, *Predictive Control With Constraints*. Upper Saddle River, NJ, USA: Prentice-Hall, 2002.

[17] J. Mattingley, Y. Wang, and S. Boyd, "Receding horizon control automatic generation of high-speed solvers," *IEEE Control Syst. Mag.*, vol. 31, no. 3, 2011.

[18] D. Q. Mayne, J. B. Rawlings, C. V. Rao, and P. O. M. Scokaert, "Constrained model predictive control: Stability and optimality," *Automatica*, vol. 36, no. 6, pp. 789–814, 2000.

[19] S. Boyd and L. Vandenberghe, *Convex Optimization*. Cambridge, U.K.: Cambridge Univ. Press, 2009.

[20] M. Grant and S. Boyd, CVX: Matlab Software for Disciplined Convex Programming (Web Page and Software) [Online]. Available: http://www.stanford.edu/~boyd/cvx/ Jul. 2008

[21] J. Mattingley and S. Boyd, CVXGEN: Automatic Convex Optimization Code Generation (web page and software) [Online]. Available: http://cvxgen.com/ Apr. 2010

[22] J. Mattingley and S. Boyd, "Real-time convex optimization in signal processing," *IEEE Signal Process. Mag.*, vol. 27, no. 3, pp. 50–61, 2010.

[23] T. Hovgaard, L. Larsen, J. Jørgensen, and S. Boyd, "Nonconvex model predictive control for commercial refrigeration," 2012.

[24] F. Allgower, R. Findeisen, and Z. K. Nagy, "Nonlinear model predictive control: From theory to application," *Journal of the Chinese Institute of Chemical Engineers*, vol. 35, no. 3, pp. 299–315, 2004.

[25] M. Cannon, "Efficient nonlinear model predictive control algorithms," *Annual Reviews in Control*, vol. 28, no. 2, pp. 229–237, 2004, Cannon, M.

[26] H. K. Alfares and M. Nazeeruddin, "Electric load forecasting: Literature survey and classification of methods," *Int. J. Syst. Sci.*, vol. 33, no. 1, 2002.

[27] V. Dordonnata, S. J. Koopmanb, and M. Ooms, "Dynamic factors in periodic time-varying regressions with an application to hourly electricity load modelling," *Comput. Stat. Data Anal.*, vol. 56, no. 11, 2012.

[28] W. Brockmann and S. Kuthe, "Different models to forecast electricity loads," 2001.

[29] P. S. C. o. N. M. (PNM), "Energy storage technology performance reports: PNM Prosperity Energy Storage Project," 2013.

[30] CAISO, CAISO Market Reports.

[31] S. Willard, "PV Plus Battery for Simultaneous Voltage Smoothing and Peak Shifting," Public Service Company of New Mexico, 2012.

[32] P. Denholm and R. M. Margolis, "Evaluating the limits of solar photovoltaics (pv) in electric power systems utilizing energy storage and other enabling technologies," *Energy Policy*, vol. 35, no. 9, pp. 4424–4433, 2007.

[33] P. Denholm and R. M. Margolis, "Evaluating the limits of solar photovoltaics (pv) in traditional electric power systems," *Energy Policy*, vol. 35, no. 5, pp. 2852–2861, 2007.

[34] E. K. Hart, E. D. Stoutenburg, and M. Z. Jacobson, "The potential of intermittent renewables to meet electric power demand: Current methods and emerging analytical techniques," *Proc. IEEE*, vol. 100, no. 2, pp. 322–334, 2012.

[35] M. Hoogwijk, D. van Vuuren, B. de Vries, and W. Turkenburg, "Exploring the impact on cost and electricity production of high penetration levels of intermittent electricity in oecd europe and the usa, results for wind energy," *Energy*, vol. 32, no. 8, pp. 1381–1402, 2007.

[36] B. K. Sovacool, "The intermittency of wind, solar, and renewable electricity generators: Technical barrier or rhetorical excuse?," *Utilities Policy*, vol. 17, no. 3–4, pp. 288–296, 2009.

[37] Allgower, F. Findeisen, and R. Nagy, in *Proc. ZK 2nd Asian Symp. Process Syst. Eng.*, Taipei, Taiwan, Dec. 04–06, 2002.

[38] Denholm, P. Margolis, and R. M., in *Proc. Int. Res. Conf. Social Acceptance Renewable Energy Innov.*, Tramelan, Switzerland, Feb. 2006.